International Journal of Global Energy Issues

ISSN online: 1741-5128 - ISSN print: 0954-7118
https://www.inderscience.com/ijgei

Automatic generation of civil engineering structure model based on network virtual reality

HaiYang Yu, Changping Chen

DOI: 10.1504/IJGEI.2023.10056391

Article History:

Received:	08 January 2022
Last revised:	18 March 2022
Accepted:	27 September 2022
Published online:	03 December 2023

Automatic generation of civil engineering structure model based on network virtual reality

HaiYang Yu and Changping Chen*

College of Ocean and Civil Engineering,
Dalian Ocean University,
Dalian, Liaoning, China
Email: yhy@dlou.edu.cn
Email: ccp@dlou.edu.cn
*Corresponding author

Abstract: The rapid development of the data age makes it closely related to research work in various fields of life. This paper uses virtual reality technology to study the automation design of civil engineering process design. Based on the traditional AR technology framework, this article combines cloud platform technology to specialise in civil engineering firmware systems. By analysing the authenticity, flexibility, regionality and high-security requirements of the fusion of virtual reality and real-time network simulation, virtual reality technology analyses the simulation network based on the cloud platform and this paper further studies the support of multiple video stream node test sites. By providing virtual reality imaging technology and actual internet connection methods, it is found that when the transmission bandwidth is between 400 Mb/s and 800 Mb/s, the packet loss rate does not exceed 0.01%. This small packet loss has almost no effect on normal network communication.

Keywords: network simulation; steel structure; three-dimensional network; cloud platform.

Reference to this paper should be made as follows: Yu, H. and Chen, C. (2024) 'Automatic generation of civil engineering structure model based on network virtual reality', *Int. J. Global Energy Issues*, Vol. 46, Nos. 1/2, pp.69–89.

Biographical notes: HaiYang Yu received the Master's degree from DaLian University of Technology, China. He studied in structural engineering. His research interests include civil engineering and structural engineering.

Changping Chen, PhD and Professor, graduated in port, coastal and offshore engineering of Dalian University of Technology in July 2010. He is currently the dean of School of Marine and Civil Engineering of Dalian Ocean University, and the professional leader of port, waterway and coastal engineering, mainly engaged in teaching and scientific research of port, waterway and coastal engineering. In recent years, he has presided over more than 20 scientific research and teaching research projects, including one general project of National Natural Science Foundation of China and eight provincial projects.

1 Introduction

With the rapid development of information technology, the internet has been integrated into all areas of life. As the fifth largest space after sea, land and air and an important national infrastructure, the security of cyberspace cannot be ignored. The emergence of virtual reality technology has had a profound impact on various fields. Using virtual civil engineering buildings in civil engineering buildings, by combining virtual reality technology with general technical courses, using three-dimensional modelling to simulate the steel structure of civil engineering buildings, the construction effect is significantly improved (Lv et al., 2017, 2019).

As the mainstream trend of existing buildings, steel-frame skyscrapers are in line with the promotion of green buildings in China, and at the same time solve the current situation of excess steel-frame industry. The application of new technologies, new processes and new materials in steel-frame high-rise buildings has led to increasing risks during the construction period. The insurance model of steel buildings directly affects the development of all risks in construction projects.

In view of the deficiencies of today's simulation technology, this article recommends virtual reality simulation technology that supports cloud platforms. Customised virtual test bed to achieve scalability, transparency, simplicity and actual virtual and virtual requirements. It can automatically push devices to promote panic and adapt to tasks. The development of civil engineering construction heralds the living standards of Chinese residents. Construction safety is more related to the life safety of residents. To improve the development level of the construction industry is to improve the happiness index of Chinese residents.

2 Related work

Network virtual technology is loved by various industries, and real scenes can be restored through network virtual reality technology. Elbamby MS's research on virtual reality headsets shows that some recipients may experience motion sickness – especially women. Among women, nearly four-fifths feel unwell (Elbamby et al., 2018). Bastug et al. (2017) emphasised the importance of VR technology as a disruptive use case of 5G (and higher) that utilises storage/memory, fog/edge computing, computer vision, artificial intelligence and other recent developments. It examines three VR case studies and provides numerical results under various storage, computing, and network configurations. It reveals the limitations of the current network, and provides reasons for more theories and innovations to lead the masses in VR (Bastug et al., 2017). Kihonge (2017) described the comprehensive process of designing 4C space mechanism in virtual environment. Virtual reality allows users to view and interact with digital models in a more intuitive way than using traditional human-machine interfaces (HCI). Network tools have the potential to greatly enhance the communication between members of different industrial site design teams (Freeman et al., 2017). Freeman et al. (2017) researched on mental health issues is inseparable from the environment. With the help of Virtual Reality (VR), a computer-generated interactive environment, individuals can

repeatedly experience their problem situations and teach how to overcome difficulties through evidence-based psychotherapy (Freeman et al., 2017). Elbamby et al. (2018) discussed the challenges and driving factors of achieving ultra-reliable low-latency VR. In addition, in the case study of the interactive VR game hall, they showed that the intelligent network design using millimetre wave communication, edge computing and active caching can realise the future vision of VR through wireless (Elbamby et al., 2018). Dascal et al. (2017) evaluated the evidence supporting the use of virtual reality in patients in acute hospitalisation settings. The research involves three general areas: pain management, eating disorders and cognitive and sports rehabilitation. Virtual reality is a promising intervention, and it has a variety of potential applications in the inpatient medical environment (Dascal et al., 2017). Kay and Asl (2017) summarised the rodent VR technology, reviewed the latest results of related research and discussed the commonalities and differences, advantages and problems of different methods. Munafo et al. (2017) reported shows that users of modern, consumer-oriented head-mounted display systems may experience motion sickness and women may face greater risks. Vankipuram et al. (2017) introduced detailed information about the framework and development methods related to the VR-based advanced cardiac life support training simulator. This is a time-critical, team-based medical scenario and it has been found that the availability score from the reduced group to the full VR group has increased (Vankipuram et al., 2017). The construction of modern civil engineering works lasts for several years, requiring a large number of personnel and types of work, various types of materials and equipment, cross-working operations have a great influence on each other and high requirements for coordination and cooperation with each other. Affected by the natural climate, many technical measures are adopted and high safety production requirements affect the construction safety and construction cycle of the project. The implementation of civil engineering construction can be improved through the network virtual reality technology.

3 The method of network virtual reality

The three technologies of physical test bed, network simulation and network simulation have their own advantages (Huang et al., 2019). Among them, the physical test bed can provide ultra-high fidelity experimental results. The network simulation technology can simulate a very large-scale target network. Network simulation technology is somewhere in between, but their respective shortcomings make it difficult for a single network reproduction technology to meet the needs of various network experiments (Gou et al., 2017). Some of the core technologies we research, such as civil engineering structure model generation technology, civil engineering structure perception technology, etc., can be extended to other environmental fields outside the physical store industry. At present, it can be foreseen that there will be applications such as clothing sales physical stores, automobile exhibition halls, etc. (Roy et al., 2017). When users experience such products online, they are not passively browsing, but can integrate into the virtual store environment and interact with the products in real time. People can go shopping and buy clothes without leaving home, or experience the driving feeling of the latest models instead of relying on imagination. The technology studied in this article can provide

effective support for new network technology research and existing network technology evaluation. The realisation diagram of the traditional AR system is shown in Figure 1. The establishment of a network system model under the traditional AR system lacks the determination and feedback of system boundaries, variables and the process of feedback analysis and correction, and lacks reliability.

Figure 1 Implementation diagram of traditional AR system

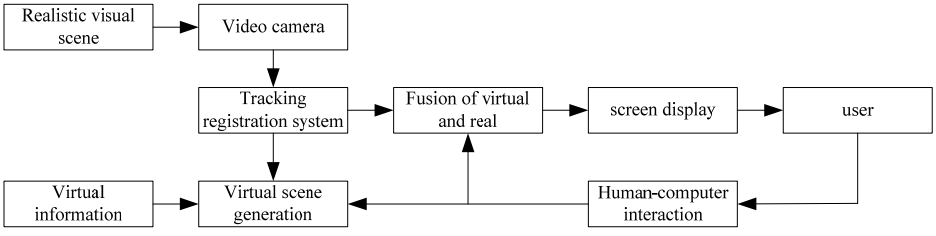

The general process of network virtual reality technology mainly includes two major steps. One is to clarify the goal of virtual reality and to construct a network model according to actual needs, and the other is to obtain data based on the constructed network model. Before modelling, it is necessary to collect research target data. In the process of modelling, not only network nodes are included, but also the connecting lines of these nodes. These connecting lines are the network systems that push each frame to match. After the modelling is completed, test inspections are carried out. Figure 2 shows a detailed network system model based on the traditional AR system. The detailed system network flow chart adds system boundaries, variable cut-offs, feedback and discussion corrections and can analyse and test for repeated experiments. Compared with the traditional AR network system, it can analyse the research object more accurately and has higher reliability.

Structural construction is to present actual problems through a network system model. The realisation of this function can be carried out according to the following process:

3.1 Clear goals and data collection

Clarify the purpose of modelling and determine the problems to be solved by the model system (Lipton et al., 2017). Based on the simulation of real objects, it is necessary to collect real data. The following is a two-dimensional plan view of photos of real objects collected by cameras, by selecting the camera angle and taking pictures at a fixed point, the resulting picture is a two-dimensional plan, as shown in the network system model diagram in Figure 3.

Figure 2 Network system model diagram

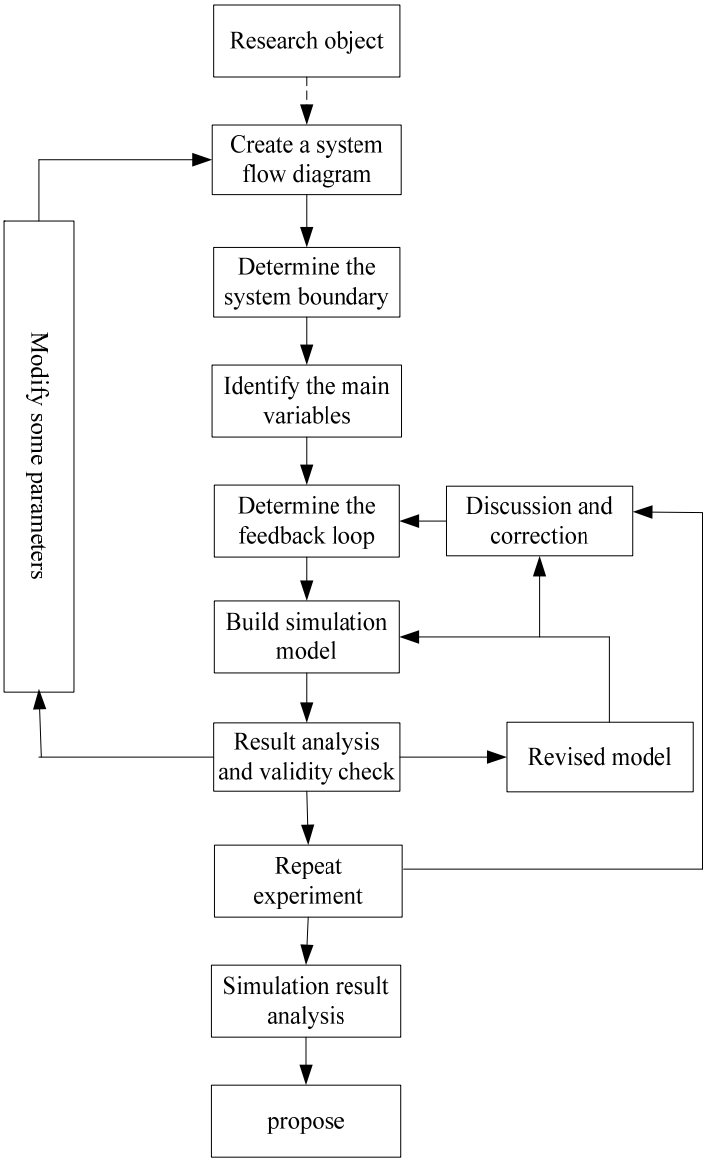

Figure 3 Two-dimensional display of real objects

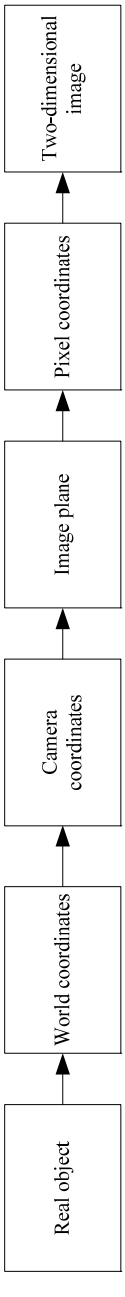

To rotate these feature points taken by the camera at fixed points, we must adhere to this principle: that is, to find the same point in the photos from different angles (Emilia et al., 2017). The criterion for selecting feature points is that these points can be easily found in the picture at every angle, and these points must also be distributed on different planes, so as to ensure that the obtained data can form a three-dimensional structure. The specific process is:

1 Use the frame data saved in the motion capture file to construct a civil engineering target structural frame. It can be called a driving frame, through which the three-dimensional building model can be promoted. The so-called three-dimensional building model refers to the three-dimensional (x, y, z) building displayed and processed through video or pictures, and entered into the detailed system network diagram.

2 The structure and shape of the driving skeleton are consistent with the original structure and shape of the three-dimensional model. In this process, we must first extract their architecture and morphological frame from the three-dimensional human body structure model, and call it the original architecture frame. After that, the two frames are overlapped, and the building frame is overlapped from the length of the building frame and the structure of the building frame.

3 Cut the building structure model according to the range that the frame nodes can influence, and divide it into different weights (Jensen et al., 2017). At the same time, in order to make this division more precise, the boundaries of each range are obtained by the building survey program. We start with the rough template model obtained in the frame fitting stage. In this stage, we will repeatedly improve the fitting accuracy by reducing the shape difference between the template and the scanned model, as shown in the figure. The shape difference found is saved to the displacement map. The main process is to obtain the video stream from the camera, extract the features of each frame and store them in the database for matching feature points and then perform tracking and matching after meeting the requirements to achieve a virtual and real-fusion state. The following is the detailed operation process, and the flowchart is shown in Figure 4.

3.2 Determine the boundary

On the basis of the research, the problems to be solved are divided and classified in the order of primary and secondary (Tkachuk et al., 2020), distinguish between system and non-system environment: System environment refers to the computer environment, that is, computer programming and non-system environment refers to the existence other than computer programming.

Figure 4 Refinement of the fitting process

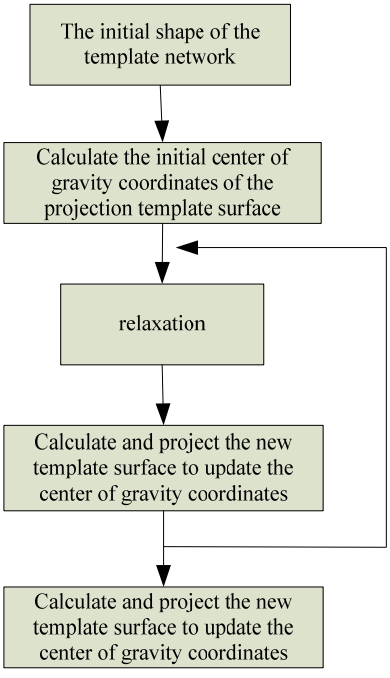

3.3 Analysis system

Analyse the relationship between the totality and sub-factors in the system, and understand the causal relationship between each element. Through the disassembly of the system, find out the connection between the various independent elements and the causal relationship between the various elements, draw them into a relationship flow diagram and present it more clearly.

1 Select the feature nodes contained in each frame of the picture in the video stream through the feature point algorithm;

2 Use the feature point description algorithm to describe the characteristic nodes in each selected picture;

3 Match the feature information obtained from the image to be matched through the feature point matching algorithm;

4 Optimise and purify the matched point pairs;

5 By purifying and correcting the mean value pair, the homography matrix is changed between the obtained feature points and then the rotation and translation matrix are performed, and finally the external parameters of the camera are solved (Kichkina et al., 2020). According to the obtained ranking, the placement position of the virtual data can be determined, so as to realise the main force position and correctly combine the virtual and real data, as shown in Figure 5.

Figure 5 Feature point detection and tracking module

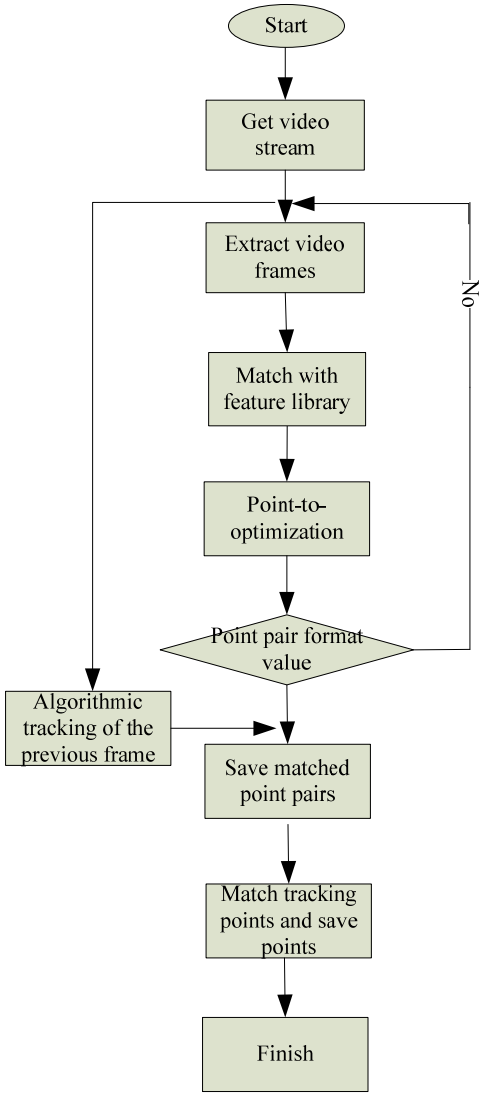

3.4 Build a model

The collected data information variables are established into functional Formulas with different mathematical methods to form a complete model. It is relied on algorithms between processes, risk network formulas, etc.

3.5 Simulation

Perform virtual simulation exercises on the constructed model to verify the effectiveness of the simulation model. In the process of simulation exercises, problems such as

unsuccessful matching, inability to select the best point and inadequate tracking are found. And through practice, continuous improvement and solutions, to find the best model program. It provides an effective policy basis for solving practical problems (Chen et al., 2021), as shown in Figure 6.

Figure 6 System structure diagram

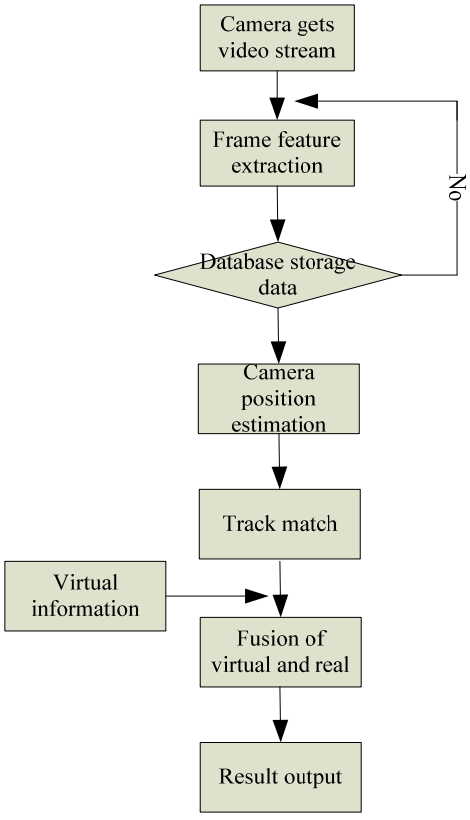

4 Automation of civil engineering structure model based on network virtual reality

4.1 The trajectory of steel structure risk propagation and the dependence path of steel structure

Discussion on the path of risk spread the spread of risk between work packages is not chaotic, but there is certain regularity, that is, they have a certain route and spread according to the trajectory. The trajectory of risk propagation depends on the dependency path between them (Wu and Li, 2020).

The project dependence between the various procedures of the steel structure high-rise building project is mainly reflected in the dependence on materials, the dependence on the work surface, the dependence on the personnel and the dependence on technology

(Lv et al., 2021). The calculation Formula for the degree of dependence between each process is as follows. The value standard in the Formula is selected strictly in accordance with the schedule arrangement, construction team arrangement and technical arrangement in the construction organisation design.

$$P = f\left(A, B, C, D\right) = \alpha A + \beta B + \chi C + \delta D \tag{1}$$

P is the degree of dependence of related processes, which represents the dependence between processes (Priyadarshi and Gupta, 2021). A indicates the relevance of materials, which is mainly reflected in the materials and components used between various processes. If the material used in the next process is the product of the previous process, it is 1, otherwise, it is 0. B represents the correlation between working surfaces, which is mainly reflected in whether this process is carried out on the basis of the previous process. If it is carried out on the basis of the previous process, it will be 1, otherwise it will be 0. C indicates the relevance of personnel, which is mainly reflected in whether the two processes use the same batch of construction personnel, management personnel and technical personnel. If it is the same group of personnel, it is 1; otherwise, it is 0. D represents the relevance of technology, which is mainly reflected in the technical relevance of the two related processes, including construction technology and management methods. The correlation is 1, if not, it is 0. Here, α, β, χ and δ represent the weight of item factors. Among them, $\alpha + \beta + \chi + \delta$ uses an n-order matrix to express the dependence between various tasks. This matrix only represents the direct dependency relationship between work packages, that is, the degree of relevance, that is, Table 1 is the structure dependency matrix. The elements other than the diagonal in the matrix are the degree of association between the various jobs to be calculated using the Formula. If there is no correlation between the two jobs, this element is 0.

Table 1 DSM structure dependency matrix

	MP1	*MP2*	...	*MPN*
MP1				
MP2				
MP3				
...				
MPN				

Based on the analysis of risk communication based on dependence, risk communication originated from the study of the dissemination of media, news and public opinion in the USA. Now combined with risk, this article explores how risk is spread. This article discusses risk spread in a narrow sense, and analyses the spread of risk factors during the construction of steel structure high-rise building projects (Goehler et al., 2020). For the establishment of the communication model, scholars have conducted research and proposed the straight-line model and the Malayzik system model from different angles. In the risk propagation analysis, the risk propagation route and propagation probability are discussed, and then the risk propagation situation is judged (Pradhan and Guha, 2020).

If the risk R1 affects MP1, then MP2 that is dependent on the work package MP1 will be affected by the risk of R1. Work packages that are dependent on MP2 MP3 will be affected by the secondary indirect propagation of R1, and WP4 that is dependent on MP3

will receive three indirect propagations. By analogy, each process is spread like this. This article takes the MP2 risk acceptance module, which has a total of 5 work packages, as an example. Figure 7 is the risk communication route of the engineering project.

Figure 7 Diagram of risk propagation route

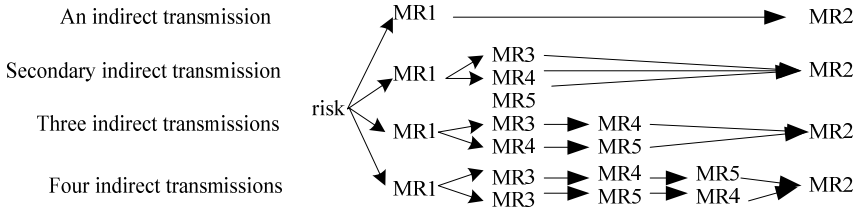

In the process of discussing the propagation path of work, the iterative propagation of risks in the workplace is ignored. That is, risk R1 affects work MP1 and MP2 depends on WP1, then R1 affects MP2. If the work of MP1 also relies on MP2, then the risk will return to MP1 and we will not consider the repeated spread of such risks. Therefore, if a project has 5 work packages, at most four indirect risk transmissions can be carried out. When we conduct theoretical research, the risk analysis of construction projects usually considers the superposition of the direct risks of each work package. In actual work, it is only the tip of the iceberg of engineering project risk and larger risk values are ignored. The risk faced by a job is the sum of the direct risk value of the job due to the direct effect of the risk and the indirect risk value of the spread of risk between jobs due to the dependency between jobs (Xiong et al., 2020). That is, project risk value = direct risk value + indirect risk value. Take MP2 work as an example, and also take 5 work packages as an example. Figure 8 shows the actual work risk of work package MP2.

Figure 8 The value of risk in the actual work of MP2

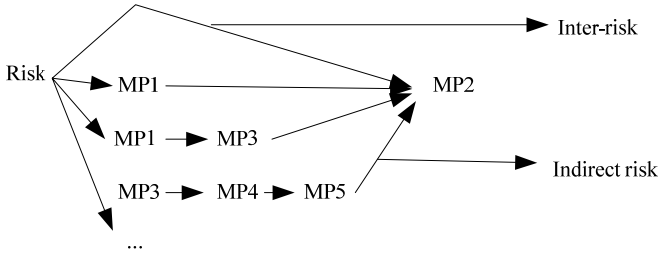

4.2 Construction of risk propagation model

In order to analyse the risks during the construction of steel structure high-rise building projects, this paper constructs a risk propagation model jointly determined by the risk network D and the risk propagation algorithm H, namely M=(D, H). Each job forms a dynamic risk network due to the spread of risks (Hou et al., 2020). Here, we first need to explore the dynamic relationship between them. D can clearly express the relationship network diagram of the risk situation. The risk propagation algorithm can accurately

calculate the propagation probability value of the work package along the dynamic risk network. Before establishing the model, it is assumed that each work package cannot resist risks and that each risk is independent (Wang et al., 2021).

The spread of risk factors, such as construction technology and management, is not limited to a single part, it is likely to spread across the structure, that is, the risk factors act on steel cutting and the risk may indirectly affect the steel structure installation project (Jiang et al., 2021). If the component size deviation is too large due to the negligence of the personnel, it may cause the deviation of the steel rod during the on-site installation of the steel structure, which will lead to the deviation of the integrity of the steel component. During the assembly process, cracks occurred in the steel due to improper construction methods. In the welding stage of the construction site, the welding operation aggravated the cracks on the rods, resulting in a reduction in the bearing capacity of the components and local collapse. In order to facilitate the discussion of risk spread, we divide the work package into modules for analysis (Choi et al., 2021; Chakraborty et al., 2021). Putting work packages that are directly related or indirectly related to the same module, no matter which work package in the module is affected by the risk event, it will be propagated to other work packages in the module. Visualising the propagation route of risk events in the work package of this module can get a risk network diagram. The risk network is formulated as:

$$D = \left(MPCW, MPCWR \right) \tag{2}$$

$$MPCW = \left\{ MPC\,W_i \middle/ MP_w, MP_n, DSW(n,w), i \le k, WP_w, WP_n \in MPCM_i \right\} \tag{3}$$

$MPCM_j$ represents a collection of coupled modules in a steel structure project. $MPCM_i$ and $MPCM_j$ are modules *i* and *j* in the project. $MPCM_i$ and $MPCM_j$ are the set of work packages that are dependent on MP_i and MP_j in the project. That is, within the work package, each work package has a direct dependence on each other.

$M\big/PCWR = \left\{ MPCWR_{ij} \middle/ MP_m, WP_n, DSM(n,m), i, j \le k, i \ne j, MP_m \in MPCW_i, WP_n \in MPCW_j \right\}$ $MPCWR$ represents the set of coupled modules, and the element $MPCWR_{ij}$ represents the module. For the impact of $MPCWR_i$ on $MPCWR_j$, this value is composed of the directly dependent value of MP_m and MP_n.

In the coupling module that divides the various construction processes of steel structures, this paper uses the correlation between the directed graph and the adjacency matrix to solve. It can judge whether the directed graph is strongly connected or weakly connected. $G = \left(V, E \right)$ represents a directed graph, where *V* represents a node of the directed graph. For this paper, *V* is the work package of the steel structure project, *E* represents the route between the nodes of the directed graph, here is the risk transmission route of each work package and the directed graph *G* is the risk network we want. The ordered pair $< v_i, v_j >$ represents the line from node v_i to node v_j. Use n-order matrix $A = \left(a_{ij} \right)$ to represent the adjacent-order matrix of the directed matrix.

$$a_{ij} = \begin{cases} 1, \text{if} < v_i, v_j > \in E, 1 \le i, j \le n \\ 0, \text{other} \end{cases} \tag{4}$$

Here, A is the Boolean DSM in the risk identification mentioned. In the directed graph G, the n-th order square matrix $P = \left(p_{ij}\right)_{n\times n}$ is the reachable matrix of the directed graph G and the algorithm is shown in Table 2.

$$P = A^{(1)} \vee A^{(2)} \vee A^{(3)} \cdots \vee A^{(n)} \tag{5}$$

$$A^{(2)} = A^{(1)} \wedge A^{(1)} \tag{6}$$

Table 2 $\wedge$ Operation rule table and $\vee$ Operation rule table algorithm table

$\wedge$	*0*	*1*
0	0	0
1	0	1
$\vee$	0	1
0	0	0
1	0	1

P is the Boolean sum of the power of A, where the elements of the matrix P are expressed as follows:

$$P_{ij} = \begin{cases} 1, v_i\ TOv_j \text{ At least one non-zero length channel exists} \\ 0, v_i\ TOv_j \text{ There are no non-zero length channels} \end{cases} \tag{7}$$

The N-order square matrix $Q = \left(q_{ij}\right)_{n\times n}$ is a strongly connected matrix of matrix P.

$$Q = P^T \cap P = \left(q_{ij}\right)_{n\times n} = \begin{bmatrix} p_{11}\times p_{11}\cdots p_{n1}\times p_{1n} \\ \cdots\cdots \\ p_{1n}\times p_{n1}\cdots p_{nm}\times p_{nn} \end{bmatrix} \tag{8}$$

According to the Boolean DSM, it is the adjacency matrix of the reachable matrix. Using the reachable matrix method to find the strongly connected matrix, we need to cluster the strongly connected matrix and finally draw the connected network diagram between the work packages according to the matrix elements.

4.3 Risk propagation algorithm

Risks are transferred between related processes. The amount of work associated with each process is different, and the number of indirect transfers received by the process is also different. The cumulative propagation probability of a process is the sum of different indirect propagation times. Use matrix A to represent the cumulative risk propagation probability matrix, and element a_{ij} to represent the work package MP_j. The probability of indirect risk spread due to the direct risk to MP_i is summed. An indirect risk spread: $d_{ij}^{(1)}$ is the direct impact value of MP_j on MP_i, and the structural dependence matrix can be searched.

Secondary indirect risk propagation: $d_{ij}^{(1)} = d_{ij}$ passes the risk to MP_k for MP_j, and MP_k passes the risk to MP_i. Here, the probability of $k \neq i \neq j$ secondary indirect risk propagation is equal to the probability that MP_i is passed to MP_k multiplied by the probability that MP_k is passed to MP_j, namely:

$$d_{ij}^{(2)} = \sum \left(d_{kj} \times d_{ij} \right), k \neq i \neq j \tag{9}$$

Three indirect risk transmission: $d_{ij}^{(3)}$ is for work, MP_j first transmits the risk to MP_m. MP_m passes the risk to MP_n, and finally MP_n passes the risk to MP_i, namely:

$$d_{ij}^{(3)} = \sum \left(d_{kj} \times d_{vk} \times d_{iv} \right), k \neq v \neq i \neq j \tag{10}$$

n–1 indirect risk transmissions: As the repeated transmission of risks is not considered, for projects with n work packages, there are at most n–1 indirect risk transmissions, namely $d_{ij}^{(n-1)}$. For the work package, the indirect risk propagation probability of MP_j to MP_i is the sum of multiple risk propagation probabilities.

$$a_{ij} = \sum_{m=1}^{n-1} d_{ij}^{m} \tag{11}$$

With this method, the risk propagation probability between each work package in the coupling module can be calculated, and the risk propagation probability matrix can be established. Each element in the matrix is the probability that the opposite work package is affected by other work packages and the risk is spread. In the process of risk spreading, the risk value does not act on the dependent process with the initial value, but is constantly decreasing. Therefore, in the process of calculating the risk propagation probability, it is only necessary to calculate the same number of indirect propagations in the coupling module. If a module contains 5 work packages, the work packages in the module only need to calculate 4 indirect risk propagations. Matrix A is the cumulative propagation probability matrix of numerical risks. The elements in the matrix are the size of the risk value when the work package encounters the corresponding risk. The following is the risk value calculation.

$$S = A \times \left(MBS - RBS \right)^T \tag{12}$$

S is the indirect risk matrix, and S_{ij} is the indirect impact value of risk events on MP_j in the indirect risk matrix S on MP_i through risk propagation. The value of each element in the S matrix is the influence of the risk on the corresponding work package due to the spread of risk.

$$T = S + \left(MBS - RBS \right)^T \tag{13}$$

T is the absolute risk matrix. The sum of the last row and the last column is the absolute risk factor of the project. According to the risk assessment of each risk and process, the risk factors and measures are classified.

$$S = \left[x, y, z \right]^T \tag{14}$$

Suppose the homogeneous coordinate of the vector X is x, and the three-dimensional homogeneous coordinate of the three-dimensional feature point is $S = \left[x, y, z, 1 \right]^T$, $A = \begin{bmatrix} \partial N_p \\ 0\ \beta_q \\ 001 \end{bmatrix}$, which is the three-dimensional coordinate transformation

matrix. $A = \begin{bmatrix} R & t \\ O^T & 1 \end{bmatrix}$ is the internal component parameter matrix used by the digital camera, and is the external component matrix obtained by marking the digital camera. $A = \begin{bmatrix} 100 \\ 010 \\ 001 \end{bmatrix}$, if the homogeneous coordinates of the contrasted image point $S = [p, q]^T$ are $S = [p, q, 1]^T$, then the relationship between them can satisfy the Formula:

$$\lambda S = AVAS \tag{15}$$

Among them: λ is a constant. According to the plan made in the previous section, the set of matching points is determined and the problem of three-dimensional reconstruction is transformed into a Jacobian problem of known matching points. The Jacobian algorithm is an algorithm that is based on the symmetric point and calculates the eigenvalues and eigenvectors of the matrix.

Assuming that the *n*-th order matrix *A* is a symmetric matrix, choose a value a_{pq} within the factors that it is not a diagonal and its absolute value should be kept to the maximum, and then use the plane torsion transformation matrix R_0^T to implement the orthogonal similar transformation Formula to *A*.

$$A_1 = R_0^T A R_0^T a_{pq} \tag{16}$$

Among them: the function of R_0 is $r_{pp} = \cos\theta; r_{qq} = \sin\theta; r_{pq} = \arcsin\theta; r_{qp} = \arccos\theta;$ $r_{ij} = 0, i, j \neq p, q$.

Calculate the angle θ according to the following Formula:

$$\tan\theta = \frac{2a_{pq}}{a_{pp} - a_{qq}} \tag{17}$$

The number $\lambda_0, \lambda_1, \lambda_2, ..., \lambda_{n-1}$ is the eigenvalue of the matrix, and the *i*-th column $(i = 0, 1, 2, ..., n-1)$ in the product of each plane rotation matrix is the eigenvector of the contrast.

Based on the discussion, using the Jacobian algorithm, the eigenvalues and eigenvectors of the *n*-th order symmetric matrix *A*, the fundamental matrix, the rotation matrix *R* and the displacement matrix *t* can be calculated respectively.

(1) If *S*=In, In is the identity matrix, then its basic matrix *n* is $n=t\times R$

(2) If the basic matrix is $n=t\times R$, then *R* can be solved by the following Formula, where: $R^T R = 1, \det R = 1$

$$\mathrm{m}tn_r = \left\| E - t \times R \right\| \tag{18}$$

(3) The most commonly used similarity estimation method is to calculate motion and engine parameters, where θ is the average correlation between motion and system parameters θ, and *X* is the correct point setting.

(4) After knowing (*R*, *t*), the coordinate value *P* of the feature point in the three-dimensional space can be calculated. The setting (m, m') is the mapping of point *P*

on the two images on the front, and the coordinate value of point *P* can be corrected by the following Formula, the parameter a_{pq} with the largest absolute value of the diagonal parameter.

$$P = ARPM1n_p\left(\|m-m\|^2 + \|m'-m'\|^2\right) \tag{19}$$

(5) Assuming that the established accuracy control parameter is ξ, if $|a| < \xi$, then the substitution calculation process ends. At this time, the diagonal parameter $a_{ij}\ (i = 0,1,2,...,n-1)$ eigenvalue λ has the same value. The eigenvector of the λ_i comparison is the *i*-th column in the matrix *S*. If $|a| \geq \xi$, then the substitution calculation process remains.

(6) Using Formulas (20), (21), (22), (23), (24), calculate the parameters in the plane transformation matrix and the parameters of the matrix *A*1 that is replaced with it.

$$x - -a_{pq}, y - \frac{1}{2}\left(a_{pq} - a_{pp}\right) \tag{20}$$

$$\mathrm{w} = \sin(y).\frac{x}{\sqrt{x^2+y^2}}, \sin 2\theta = w \tag{21}$$

$$\begin{cases} \sin\theta = \dfrac{w}{\sqrt{2(1+w^2}} \\ \cos\theta = \sqrt{1-\sin^2\theta} \end{cases} \tag{22}$$

$$\begin{cases} a_{pp}^{(1)} = a_{pp}\cos^2\theta + a_{qq}\sin^2\theta + a_{pq}\cos 2\theta \\ a_{qq}^{(1)} = a_{pp}\sin^2\theta + a_{qq}\cos^2\theta + a_{pq}\sin 2\theta \end{cases} \tag{23}$$

$$a_{pp}^{(1)} = a_{pq}^{(1)} = 0, \begin{cases} a_{pj}^{(1)} = a_{pj}\cos\theta + a_{qj}\sin\theta, \\ a_{pj}^{(1)} = -a_{pj}\sin\theta + a_{qj}\cos\theta, \\ a_{tp}^{(1)} = a_{tp}\cos\theta + a_{tp}\sin\theta, \\ a_{tq}^{(1)} = -a_{tp}\sin\theta + a_{tp}\cos\theta, \end{cases} \tag{24}$$

(7) Repeat steps (4)–(6) to calculate.

Steps (1) and (2) are transformation matrix problems, which should be solved using the Quaternion-Representation method. Steps (3), (4), (5), (6) are non-linear minimisation problems, which should be solved using the Levenberg-Marquardt method to obtain a grid structure composed of characteristic points BV coordinates.

4.4 Scalability and network performance test and result analysis

First, test the throughput inside the virtual network. Since the container is added in this chapter, the throughput of the container needs to be tested. The internal throughput of the virtual network refers to the maximum rate at which the device can operate without losing frames in the video stream, that is, the maximum rate test of the virtual network system. The test results show that the throughput between containers connected to the same virtual network is 7893.67 Mb/s, which shows that the network card in the

container limits the throughput to gigabit. After adding a container-based virtual router between the two containers, the throughput is reduced to less than 1000 Mb/s. It can be seen that the container router has a relatively large impact on the throughput. Therefore, VM-based virtual routers are selected to provide routing services in subsequent performance tests. Each test result is a value obtained after 6 tests. Since the network card used in the test only supports Gigabit networks, the test results of real and virtual networks should be around 1000 Mb/s. When the transmitter bandwidth is between 400 Mb/s and 800 Mb/s, the packet loss rate does not exceed 0.01%. This small packet loss has almost no impact on standard networks. The amount of packet loss is obvious, and it is actually 800 Mb/s. Although the rapid increase of modern network users has reduced the transmission bandwidth, it can still achieve high-transmission bandwidth while maintaining low data packet value, as shown in Figures 9 and 10.

Figure 9 Throughput test results delay test results (see online version for colours)

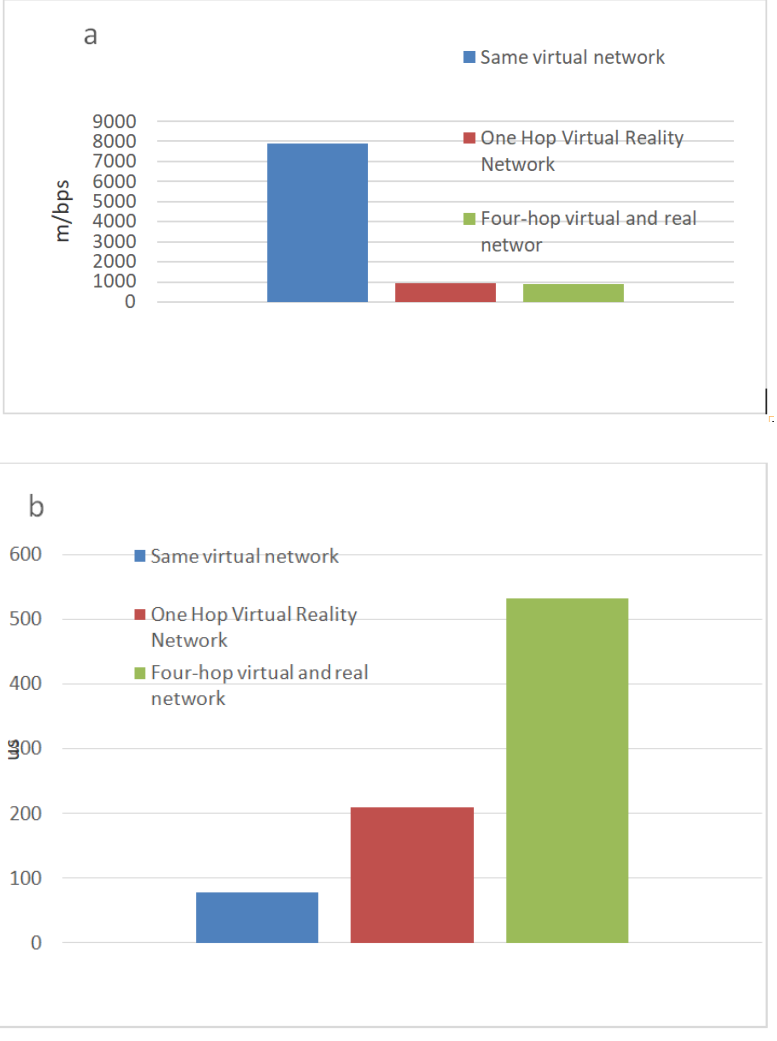

Figure 10 Packet loss rate test results (see online version for colours)

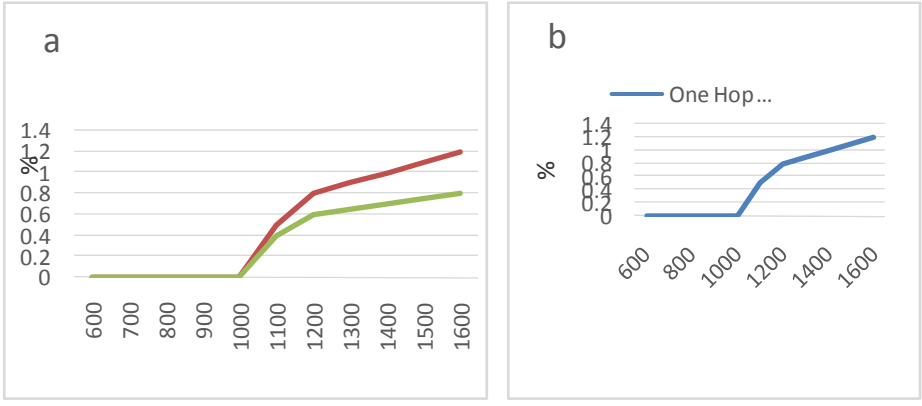

From the three experiments conducted on the three networks, the modern real-time cloud broadcasting technology based on the cloud system outlined in this article can build a more efficient and functional environment.

5 Discussion

Based on the traditional AR system model to refine and form a new network model, establish feature points and tracking modules, establish a simulation model and improve through practice to find the best model. In the established simulation model, the feasibility and scalability of the network are tested by packet loss rate test. The test results show that the reliability of the network simulation model is high, and it can be applied in the research of civil engineering construction.

The network virtual reality technology uses software systems, database systems and hardware systems to simulate private environments on virtual servers to generate integrated physical experiments that can listen, touch and watch. In future research, taking into account the application expectations, we will also focus on the overall development of high-tech technology.

6 Conclusions

Network virtual reality technology uses computer resources to simulate multiple independent virtual computing environments, namely virtual machines, on a physical server. These virtual machines can not only participate in communication as terminal hosts, but also serve as virtual switches and virtual routers to build large-scale simulation networks. Because network virtual reality technology uses virtual resources to simulate a complete network environment, although it cannot be compared with network simulation in scale, it can effectively support the accurate evaluation of operating systems, network protocols and kernels. Therefore, it has become the mainstream technology of network experiment and effect evaluation platform.

References

Bastug, E., Bennis, M. and Medard, M. et al. (2017) 'Toward interconnected virtual reality: opportunities, challenges, and enablers', *IEEE Communications Magazine*, Vol. 55, No. 6, pp.110–117.

Chakraborty, A., Jindal, M. and Khosravi, M.R. et al. (2021) 'A secure IoT-based cloud platform selection using entropy distance approach and fuzzy set theory', *Wireless Communications and Mobile Computing*, No. 9, pp.1–11.

Chen, J., Wang, Y. and Zhan, X. (2021) 'Topology optimization of steel structure for waste incineration steam generator based on DE and PSO', *International Journal of Steel Structures*, Vol. 21, No. 4, pp.1210–1227.

Choi, S., Woo, J. and Yang, H.P. et al. (2021) 'User-friendly method of digital twin application based on cloud platform for smart manufacturing', *Transactions of the Korean Society of Mechanical Engineers A*, Vol. 45, No. 2, pp.175–184.

Dascal, J., Reid, M. and Ishak, W.W. et al. (2017) 'Virtual reality and medical inpatients: a systematic review of randomized, controlled trials', *Innovations in Clinical Neuroscience*, Vol. 14, Nos. 1/2, pp.14–21.

Elbamby, M.S., Perfecto, C. and Bennis, M. et al. (2018) 'Towards low-latency and ultra-reliable virtual reality', *IEEE Network*, Vol. 32, No. 2, pp.78–84.

Emilia, B., Elena, B. and Ambra, C. et al. (2017) 'An immersive virtual reality platform to enhance walking ability of children with acquired brain injuries', *Methods of Information in Medicine*, Vol. 56, No. 2, pp.119–126.

Freeman, D., Reeve, S. and Robinson, A. et al. (2017) 'Virtual reality in the assessment, understanding, and treatment of mental health disorders', *Psychological Medicine*, Vol. 47, No. 14, pp.1–8.

Goehler, A., Harry Hsu, T-M., Tmhh, C. and Lacson, D.R. et al. (2020) 'Three-dimensional neural network to automatically assess liver tumor burden change on consecutive liver MRIs – ScienceDirect', *Journal of the American College of Radiology*, Vol. 17, No. 11, pp.1475–1484.

Gou, F., Chen, H. and Li, M.C. et al. (2017) 'Submillisecond-response liquid crystal for high-resolution virtual reality displays', *Optics Express*, Vol. 25, No. 7, pp.7984–7997.

Hou, Q., Xing, Y. and Wang, D. et al. (2020) 'Study on coupling degree of rail transit capacity and land use based on multivariate data from cloud platform', *Journal of Cloud Computing*, Vol. 9, No. 1, pp.1–12.

Huang, Y., Sheng, W., Jin, P., Nie, B., Qiu, M. and Xu, G. (2019) 'A node-oriented discrete event scheduling algorithm based on finite resource model', *Journal of Organizational and End User Computing (JOEUC)*, Vol. 31, No. 3, pp.67–82. Doi: 10.4018/JOEUC.2019070104.

Jensen, K., Bjerrum, F. and Hansen, H.J. et al. (2017) 'Using virtual reality simulation to assess competence in video-assisted thoracoscopic surgery (VATS) lobectomy', *Surgical Endoscopy*, Vol. 31, No. 6, pp.1–9.

Jiang, W., Li, Z. and Zhang, S. et al. (2021) 'Hydraulic pump fault diagnosis method based on EWT decomposition denoising and deep learning on cloud platform', *Shock and Vibration*, No. 8, pp.1–18.

Kay, T. and Asl, A. (2017) 'Virtual reality systems for rodents', *Current Zoology*, No. 1, pp.109–119.

Kichkina, A.A., Matrosov, M.Y. and Fron, L.I. et al. (2020) 'M/A-constituent in bainitic low-carbon high-strength steel structure: Part 2', *Metallurgist*, Vol. 63, No. 11, pp.1266–1279.

Kihonge, J.N. (2017) 'Spatial mechanism design in virtual reality with networking', *Journal of Mechanical Design*, Vol. 124, No. 3, pp.435-440.

Lipton, J.I., Fay, A.J. and Rus, D. (2017) 'Baxter's homunculus: virtual reality spaces for teleoperation in manufacturing', *IEEE Robotics and Automation Letters*, Vol. 3, No. 1, pp.179–186.

Lv, Z., Chen., D., Lou, R. and Alazaab, A. (2021) 'Artificial intelligence for securing industrial-based cyber-physical systems', *Future Generation Computer Systems*, Vol. 117, pp.291–298.

Lv, Z., Li, X. and Li, W. (2017) 'Virtual reality geographical interactive scene semantics research for immersive geography learning', *Neurocomputing*, Vol. 254, pp.71–78.

Lv, Z., Li, X., Lv, H. and Xiu, W. (n.d.) 'BIM big data storage in WebVRGIS', *IEEE Transactions on Industrial Informatics*, Vol. 16, No. 4, pp.2566–2573.

Munafo, J., Diedrick, M. and Stoffregen, T.A. (2017) 'The virtual reality head-mounted display oculus rift induces motion sickness and is sexist in its effects', *Experimental Brain Research*, Vol. 235, No. 3, pp.889–901.

Pradhan, K. and Guha, A. (2020) 'A systematic study of blockage in three-dimensional branching networks with an application to model human bronchial tree', *Theoretical and Computational Fluid Dynamics*, Vol. 34, pp.1–32.

Priyadarshi, R. and Gupta, B. (2021) 'Area coverage optimization in three-dimensional wireless sensor network', *Wireless Personal Communications*, Vol. 117, No. 2, pp.843–865.

Roy, E., Bakr, M.M. and George, R. (2017) 'The need for virtual reality simulators in dental education: a review', *Saudi Dental Journal*, Vol. 29, No. 2, pp.41–47.

Tkachuk, M.A., Golovin, S.V. and Fron, L.I. et al. (2020) 'Effect of alloying with molybdenum and chromium on low-carbon pipe steel structure and properties', *Metallurgist*, Vol. 63, No. 9, pp.1043–1053.

Vankipuram, A., Khanal, P. and Ashby, A. et al. (2017) 'Design and development of a virtual reality simulator for advanced cardiac life support training', *IEEE Journal of Biomedical and Health Informatics*, Vol. 18, No. 4, pp.1478–1484.

Wang, D., Lv, X. and Zhang, S. et al. (2021) 'Role of network cloud platform-based and progressive health education in postoperative rehabilitation of patients with tibial fracture', *American Journal of Translational Research*, Vol. 13, No. 5, pp.4819–4824.

Wu, W. and Li, X. (2020) 'Lateral stress characteristics of steel structure wall module exerted by self-compacting concrete', *Iranian Journal of Science and Technology – Transactions of Civil Engineering*, Vol. 44, No. Suppl 1, pp.79–89.

Xiong, C., Xiang, R. and Li, Y. et al. (2020) 'RETRACTED ARTICLE: large-scale image-based fog detection based on cloud platform', *Multimedia Tools and Applications*, Vol. 79, No. 13, pp.9663–9663.